The 8th International Supercritical CO_2 Power Cycles Symposium
February 27 – 29, 2024, San Antonio, Texas
Paper #105

STEP 10 MWe SCO_2 Turbine Design, Assembly and Commissioning

Jeffrey Moore, Ph.D.
Institute Engineer
Southwest Research Institute
San Antonio, TX

John Klaerner
Research Engineer
Southwest Research Institute
San Antonio, TX

Jonathon Wade
Manager, Power Cycle Machinery
Southwest Research Institute
San Antonio, TX

Jason Mortzheim
GE Research
Niskayuna, NY

Giridhar Jothiprasad, Ph.D.
Principal Engineer
GE Research
Niskayuna, NY

Dr. Jeffrey Moore is an Institute Engineer in the Machinery Section at Southwest Research Institute in San Antonio, TX. He holds a B.S., M.S., and Ph.D. in Mechanical Engineering from Texas A&M University. His professional experience includes Solar Turbines Inc. in San Diego, CA, Dresser-Rand in Olean, NY, and Southwest Research Institute in San Antonio, TX. He is the co-PI for the STEP project and has authored over 50 technical papers related to turbomachinery, co-authored four book chapters related to compression, sCO2 power cycles, energy storage, and hydrogen machinery, and has five patents issued.

Mr. John Klaerner is a Research Engineer in the Rotating Machinery Dynamics Section at Southwest Research Institute® in San Antonio, Texas. He holds a B.S. in Mechanical Engineering from Texas A&M University where he began his studies of large machinery and various power systems. His professional experience at SwRI has allowed for continuing in machinery design and thermal analysis, mostly related to equipment being used in Supercritical Carbon Dioxide (sCO2) cycles. These focuses have led to further experience in instrumentation, commissioning, and testing of individual cycle components, full sCO2 test loops, and other energy storage programs.

Mr. Jonathan Wade is a manager in the Power Cycle Machinery Section at Southwest Research Institute in San Antonio, Texas. He holds a B.S. and M.S. in Mechanical Engineering from Texas A&M University, he has over 20 years of experience working with turbomachinery. His research interests are in the areas of turbomachinery rotordynamics, seals, bearings, foil gas bearings, microturbines, structural dynamics, finite element analysis, and fluid-structure interactions. He is experienced in turbomachinery design, high-vibration (synchronous and sub-synchronous) root cause and corrective action investigations, machine failure investigations, and vibration and performance testing.

Mr. Jason Mortzheim is a senior mechanical engineer at the GE Global Research Center in Niskayuna, NY. He has a B.S. in aeronautical engineering from Rensselaer Polytechnic Institute and a M.S. in aerospace engineering from Georgia Institute of Technology. His area of research has been centered on improving fossil power combined cycle plant efficiency including both steam and gas turbines. Mr. Mortzheim initial area of research focused around advanced seal designs where he has held various roles spanning his 21 year professional career. He has utilized computational methods, both commercial CFD and in-house flow solvers, advanced experimental campaigns including industry leading test rig designs, complete to post commercial operation validation to develop state of the art seal technology ranging from brush seals to film riding seals.

Dr. Giridhar Jothiprasad is a principal engineer at the GE Global Research Center in Niskayuna, NY. His research involves the aerodynamic analysis and modeling of turbo-machinery flows. He completed his doctoral studies at Cornell University. developing a framework for error-control in large eddy simulation. At GE, he has been involved in aerodynamics projects that improve compressor performance and operability. He has supported the aero design of radial compressors for various advanced applications: mobile power generation, supercritical CO2 cycles and advanced Brayton cooling for next-gen aircraft engines. Dr. Jothiprasad has co-authored over 11 research papers in peer-reviewed journals and conference papers and has won the prestigious Olin and Sage fellowships for graduate study at Cornell University. Lockheed Martin awarded the "Excellence in Research Award for GE" for his flow control work.

ABSTRACT

The sCO2 turbine used in the Supercritical Transformational Electric Power (STEP) Demo pilot plant, which is a 10 MW supercritical carbon dioxide (sCO2) test facility located at Southwest Research Institute (SwRI) in San Antonio, has been assembled, and initial commissioning of the turbine subsystems has been performed. The project was developed in partnership with GTI Energy and GE Research and is sponsored by the U.S. Department of Energy (DOE) as part of the $169 million STEP Demo project. The turbine has a 16 MW output yet weighs only 90 kg, making it the highest power density of any industrial turbine. This paper describes the turbine design, construction, and assembly, as well as the installation of the turbine skid, piping, and wiring. Preliminary commissioning of the turbine skid is described, including pipe connections, alignment, and commissioning of ancillaries like the dry gas seal supply panel and the lubrication oil system.

INTRODUCTION

sCO2 power cycles have received significant interest and development through both commercial and government-sponsored efforts due to the potentially greater thermodynamic efficiency, small equipment size, and relative safety of CO2 as the working fluid. The cycle reduces capital costs due to the smaller footprint of the equipment. Lower thermal mass permits faster thermal cycles, allowing the power plant to follow the highly cyclic demand of the future electrical grid due to variable renewable energy.

A team led by Gas Technology Institute (GTI®), Southwest Research Institute® (SwRI®), and General Electric Global Research (GE-GR) is executing a project called "STEP" [Supercritical Transformational Electric Power Project], to design, construct, commission, and operate a 10 MWe supercritical CO2 pilot plant test facility. The $156 million project is 80% funded by the US DOE's National Energy Technology Laboratory (NETL Award Number DE-FE0028979), with the remaining 20% by team members, component suppliers, and others interested in sCO2

technology. The facility is currently under construction and is located at SwRI's San Antonio, Texas, USA, campus. This project is significant in technology readiness level (TRL) for indirect sCO2 cycle-based power generation commercialization and is providing vital data on the performance, operability, and scale-up of commercial plants (Marion, et al., 2020). The cycle was optimized and presented by McClung, et al., 2018.

At the heart of the plant is the sCO2 turbine developed jointly by SwRI and GE Research. It represents the highest power density of any industrial turbine providing over 16 MW gross power while weighing less than 80 kg. It is based on the earlier prototype developed under the Sunshot program, which was tested at SwRI under full temperature, pressure, and speed conditions in an earlier 1 MW test loop (Moore, et al., 2015, 2018 and 2020). This important develop program retired many of the risks related to thermal management, use of dry gas seals in SCO2, bearing design, rotordynamics, pressure containment, loop design, and the first use of Inconel 740H for piping and heat exchangers. The learnings were incorporated into the STEP turbine design as will be described below. The aeromechanical design of the STEP Turbine was described by Cich, et al. (2018).

TURBINE DESIGN

The power cycle for the facility was set to run at turbine inlet conditions of 715°C (1319°F) and 250 bar (3626 psi). The final design of the pressure casing was set to 280 bar and 720°C. A turbine with these conditions was designed and set to produce 16 MW gross in order to power the bypass compressor on the turbine train as well as cover the electric load of the AC motor and VFD setup driving the compressor. *Figure 1* provides a cross-section of the turbine along with design limits for pressure, temperature, speed, and life.

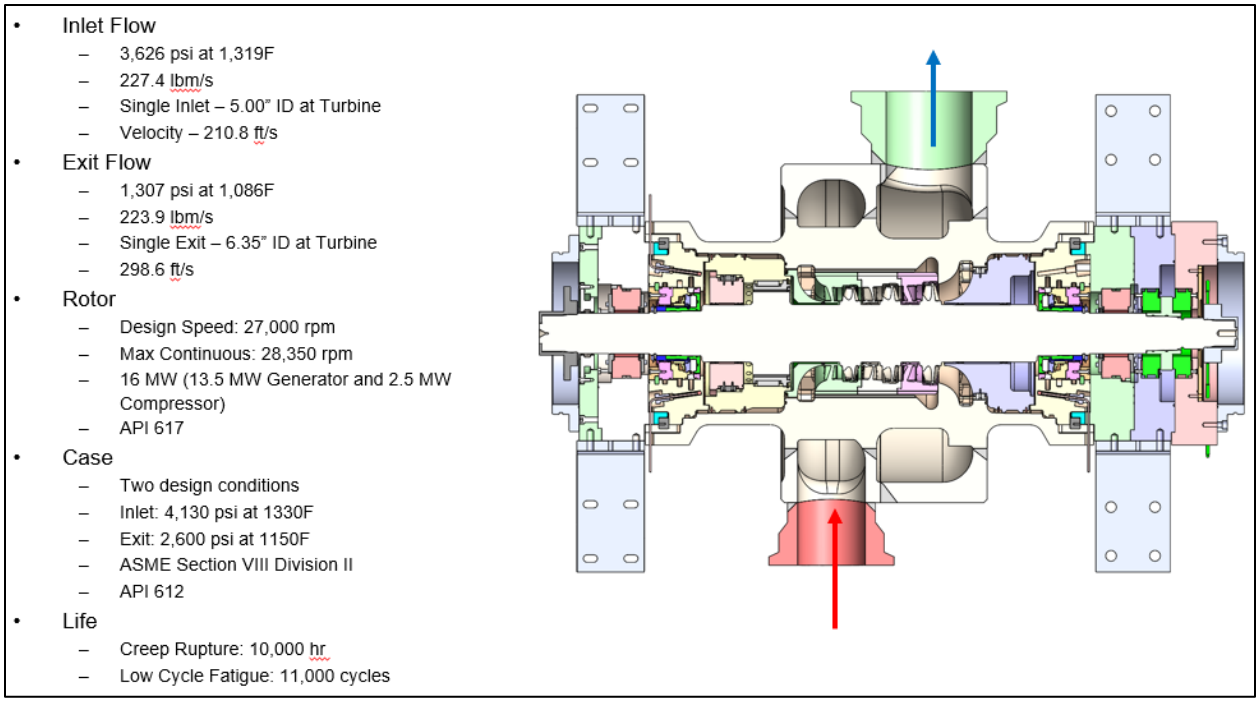

Figure 1 Section view illustration of the STEP Turbine with design conditions

Figure 2 shows the major components in the turbine design consisting of a 3-stage axial flow turbine, dry gas seals (DGS), tilt-pad journal and thrust bearings, and flexible couplings on each end driving the bypass compressor on one end and the gearbox/generator on the other. A rotordynamics model was developed to predict the natural frequencies of the machine to place those away from the 27,000 rpm design speed. Significant time was spent developing the casing geometry, pressure containment, and thermal management system to balance all loads on the unit. With the use of dry gas seals, a significant temperature reduction is needed in the process flow portion of the unit. The maximum temperature for the DGS area is 200°C, and the bearings must be even cooler. Many design iterations were conducted optimize the performance, rotordynamics, pressure containment, and thermal management., several.

In order to accommodate the high blade loading while maintaining maximum hub diameter of the shaft for rotordynamic purposes, integral blades with the shaft were required. This concept was originally implemented in the Sunshot turbine, but with full-height blades on the STEP design. Machining with 5-axis electrode discharge machining (EDM) was employed with specially shaped electrodes to make the integral shaft, blade, and shroud 3-stage design.

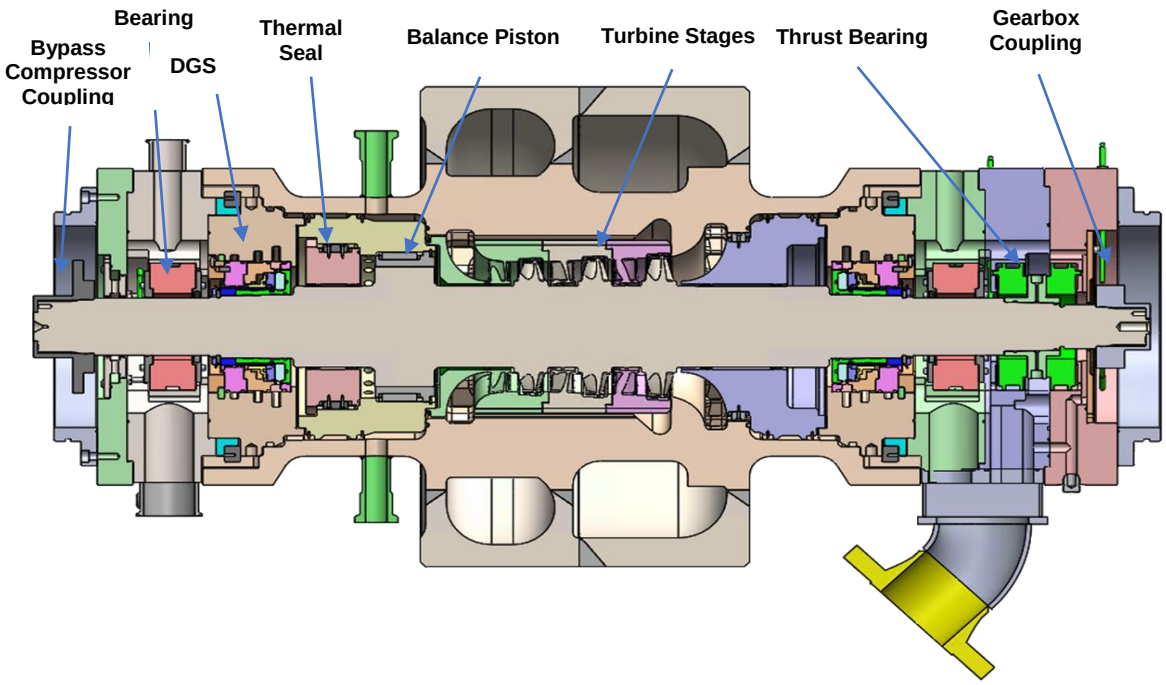

Figure 2 - Cross-section of the STEP Turbine

CASE DESIGN

The Sunshot casing consisted of an axially stacked design to simplify the casting shapes. The final concept used a fabricated design, which was adopted into the STEP design but with a single-piece casing. The inner barrel of the casing is monolithic, with flow passages being accommodated using struts through the flow path, as shown in

Figure 3. The plenums are welded onto the main case along with the nozzles to create the inlet and exit plenums using full penetration welds.

The case design is driven by thermal loads experienced during startup and shutdown. An excessive temperature rate increase or decrease can generate significant thermal stresses in the rotor and casing. This part of the turbine design required extensive effort as the team wanted to make sure the turbine was not the limiting factor in the plant rate of the plant temperature but also needed to provide adequate time for warming without distorting. When working with a room-temperature pressure vessel, material thickness is the key factor and increases along with pressure. The key factor with high-temperature vessels is that thick material creates higher thermal stresses in the vessel walls than a thinner vessel would. Hence, high-pressure and high-temperature pressure vessels must be designed with that compromise in mind.

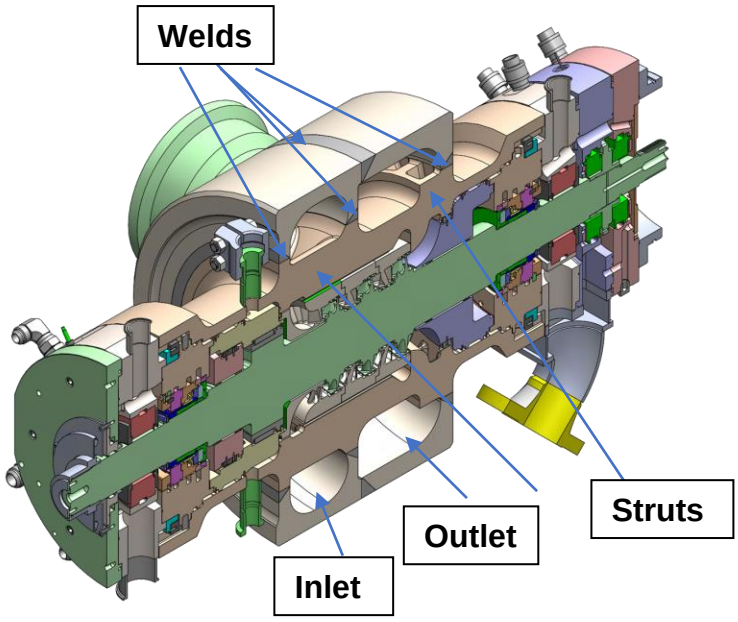

Figure 3 - Isometric View of STEP Case Showing Weld Placement

ROTORDYNAMICS

A detailed lateral rotordynamic analysis was conducted for the STEP turbine, including an undamped critical speed (UCS) analysis, damped unbalance response calculations, and rotordynamic stability analysis. Several iterations of lateral rotordynamic calculations were performed during the mechanical and rotordynamic design of the turbine. Major aspects that influenced the lateral rotordynamics include the rotor design, tilting-pad journal bearings with integral squeeze-film dampers (ISFDs), hole-pattern balance piston seal design, coupling design, casing design, and support flexibility.

Figure 4 provides the final STEP turbine lateral rotor model. This beam element rotor model includes the turbine rotor, journal bearings with ISFDs, representative beam element casing, and pedestal stiffness connections to the ground. The rotor material properties, especially modulus of elasticity, are adjusted for the hot section of the turbine, as shown by the red versus gray elements

in Figure 4. The coupling half-weights, dry gas seals, and turbine stages are modelled as discrete added masses at the appropriate locations on the rotor. The journal bearings are modelled with the fluid-film and ISFD stiffness and damping coefficients between the rotor and the case. The damping from the ISFDs was measured experimentally by Ertas, Delgado, and Moore (2018). A beam element casing model is included via yellow elements with added masses to capture the case mass and inertia properties. This beam element casing model accounts for the rigid-body casing dynamics and its influence on the lateral rotordynamics. It is noted that this beam element representation of the case is not meant to properly model the casing bending modes, which are covered separately in the casing finite element analysis (FEA). The pedestal stiffness values were also derived from a casing FEA and applied to the rotor model to connect the beam element casing model to ground. Figure 5 shows the pedestal stiffness used in the model as predicted with FEA.

The undamped critical speed map for the STEP turbine is shown below in Figure 6. For the undamped analysis, the ISFD stiffness is held at a constant value, and the undamped critical speeds are calculated for a varying fluid-film stiffness at the journal bearings without the influence of damping. The direct stiffness versus speed of the bearing fluid-film for minimum and maximum clearance are overlaid on the UCS map. As indicated in Figure 6, the turbine rotor is predicted to operate above the first three rotor modes, including the first bending rotor mode, as well as above the rigid body casing modes. The fourth rotor mode, or second bending mode, is predicted above running speed at approximately 35 krpm. The predicted undamped critical speeds are not very sensitive to bearing stiffness, which is expected since the stiffness of the ISFD is the controlling spring of the rotor system. Overall, good separation is noted between the operating speed and the bending rotor modes. Figure 7 provides representative mode shapes corresponding to the undamped critical speeds, including both cylindrical and conical rotor and casing modes, as well as rotor bending modes.

A damped response analysis was conducted to evaluate the rotor vibration sensitivity to mechanical unbalance. This analysis assumes an API unbalance is applied to the rotor in configurations to excite the potential lateral modes of interest. These unbalance response calculations are performed for both minimum and maximum clearance conditions. Figure 8 presents representative lateral response predictions at the journal bearings for a mid-span unbalance simulating the excitation of cylindrical modes. Similarly, Figure 9 provides the unbalance response for the journal bearings for an out-of-phase unbalance placed on each end to excite conical modes. The notable peak responses below 10 krpm are casing modes that are excited by the unbalance. While casing modes are predicted to have high amplification, the response levels are relatively low (well below 1 mil, p-p). The first three rotor modes are well-damped due to the ISFDs, and the corresponding responses are not noticeable with the presence of casing modes. The fourth rotor mode (or second bending) is highly amplified above running speed when approaching 35 krpm. Overall, the predicted unbalance response vibration levels and separation margins are considered acceptable and meet API 617 guidelines (API, 2014).

A rotordynamic stability analysis was also performed, including the calculation of damped natural frequencies and logarithmic decrements (log dec) to evaluate stability. While the stability results are not shown here, the analysis is described here briefly. The stability analysis includes the full stiffness and damping effects of the journal bearings, ISFDs, hole-pattern balance piston seal, and the destabilizing aerodynamic cross-coupling from the turbine stages. The predicted log dec results are calculated for increasing applied cross-coupled stiffness, or Kxy, to evaluate the

sensitivity of the rotor system to destabilizing forces. The stability analysis for the STEP turbine predicted high log dec values above 1.0 with good stability margins. The stability analysis also included an evaluation of the sensitivity of the seal clearance taper, including converging and diverging clearances, for the hole-pattern balance piston seal. The effective damping of hole-pattern seals is highly dependent on the clearance taper, and this evaluation is crucial to ensuring stable design. The hole-pattern balance piston seal for the STEP turbine is designed to have a converging taper with a predictable level of effective damping and favorable rotordynamic stability.

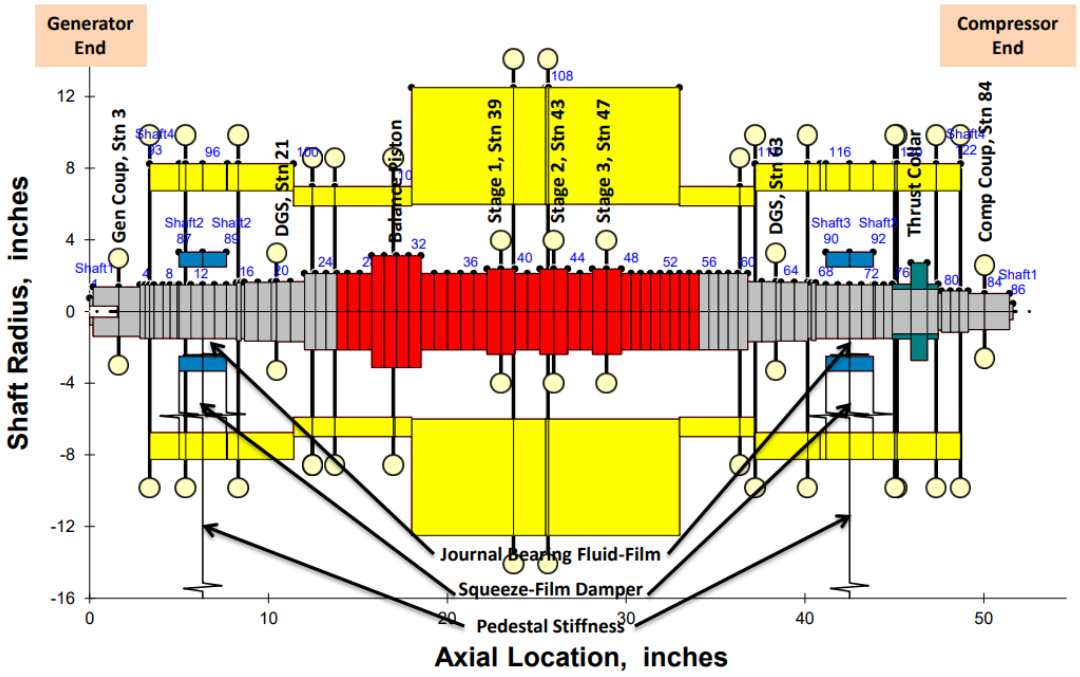

Figure 4 - STEP Turbine Lateral Rotordynamic Model

GB End Pedestal Stiffness (Individual)		
Axis	k (lbf/in)	
x	0	
y	904,975	Kyy
z	895,725	Kxx

Comp End Pedestal Stiffness (Individual)		
Axis	k (lbf/in)	
x	411,875	
y	904,975	Kyy
z	895,725	Kxx

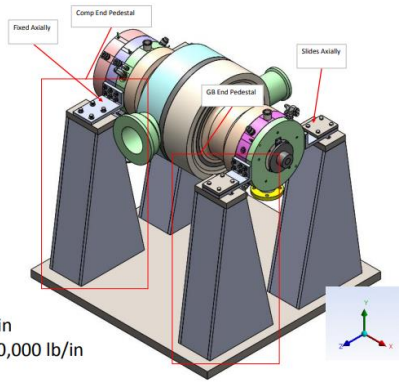

Ki = individual pedestal = ~900,000 lb/in
Kped = per bearing end = 2*Ki = ~1,800,000 lb/in

14

Figure 5 - Pedestal Stiffness used in Rotordynamics Model Predicted by FEA

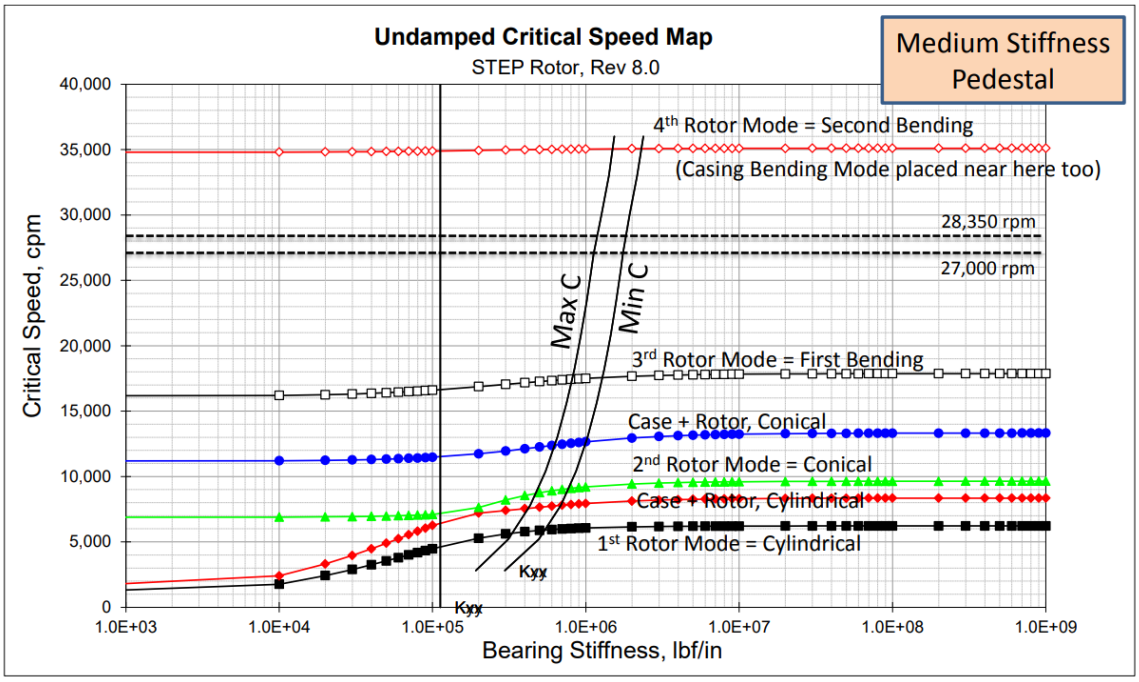

Figure 6 - STEP Turbine Undamped Critical Speed Map.

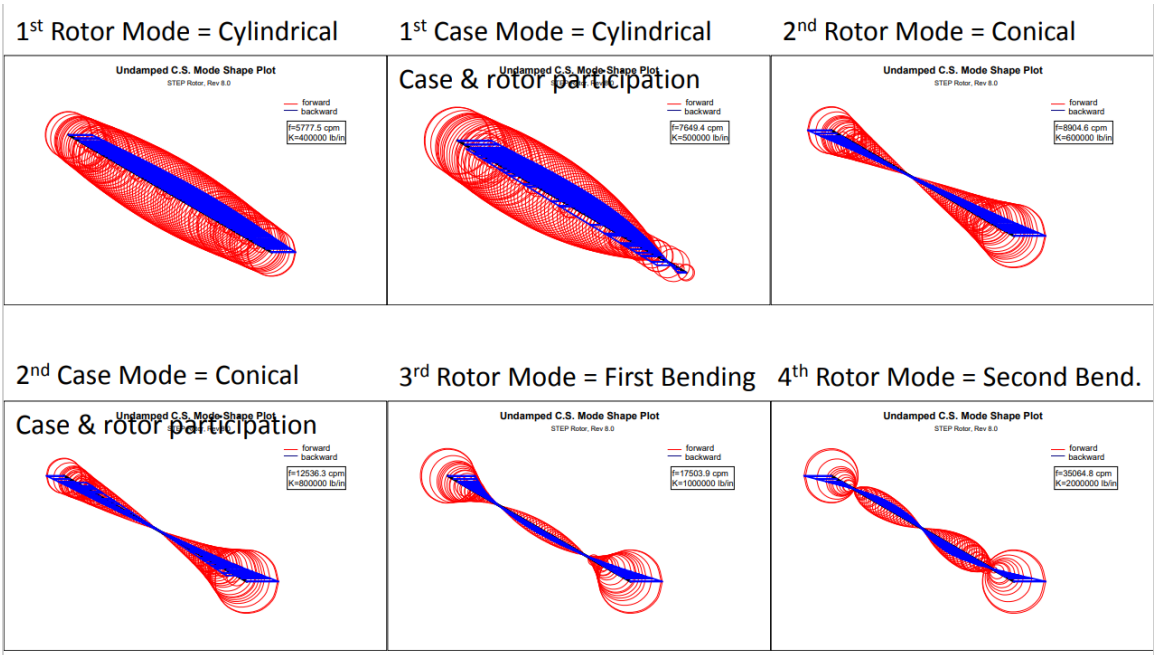

Figure 7 - STEP Turbine Representative Undamped Mode Shapes, Including Rotor and Rigid Casing Modes.

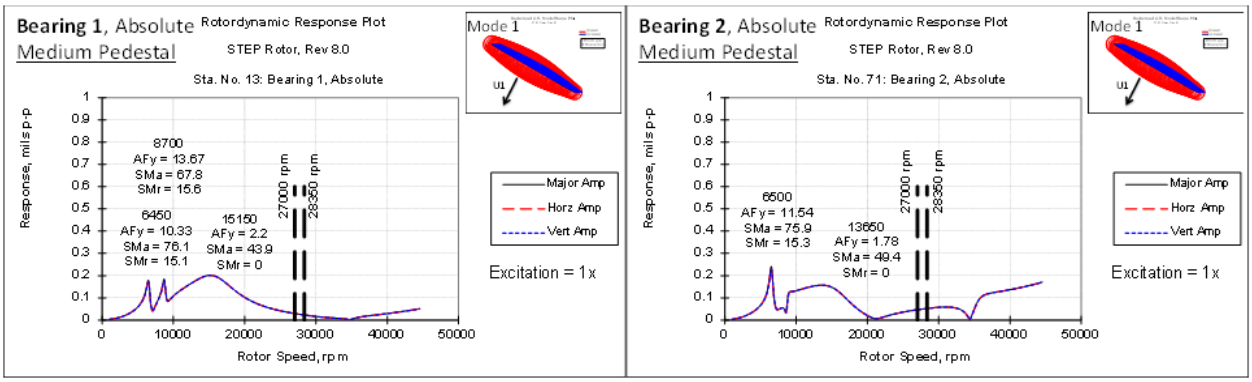

Figure 8 - STEP Turbine Predicted Lateral Response at Journal Bearing Unbalance Applied Mid-Span Unbalance

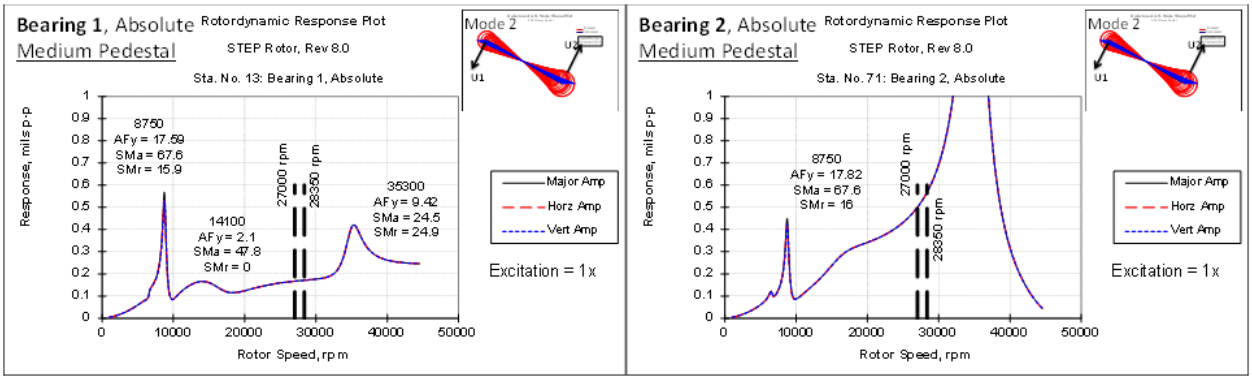

Figure 9 - STEP Turbine Predicted Lateral Response at Journal Unbalance Applied to Both Ends Out-Of-Phase

CASE DYNAMICS

With the completed turbine design, a pedestal was designed to place the casing modes away from the operating speed range. The rigid body modes of the casing were placed well below running speed by tuning the design of the L-brackets connecting the casing to the pedestals. The casing bending modes are all placed well above the operation speed. Figure 10 below shows the FEA predicted modes of the turbine while on the stand. These frequencies will be confirmed by modal testing later in this paper.

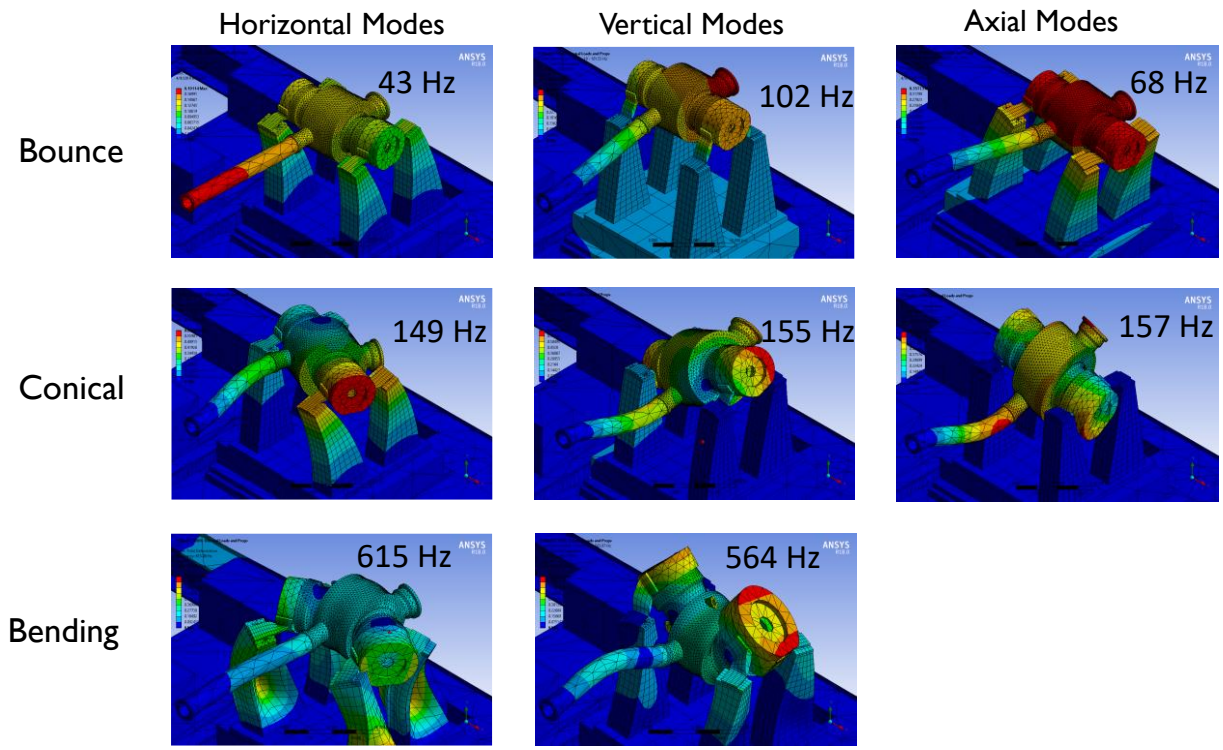

Figure 10 - Turbine Case Predicted Natural Frequencies and Mode Shapes using FEA

CASING MANUFACTURING

The casing was designed to accommodate 265 bar, 715°C inlet conditions in accordance with ASME Boiler and Pressure Vessel Code, Section VIII, Division 2 [ASME, 2019] using Inconel 625, which provided adequate life for the test program (10,000+ hour life). Transient finite element analysis (FEA) was used to optimize the case design for relatively fast start-ups and shutdowns so that it would not limit transient plant operation. Commercial embodiments will be made from either Inconel 740H or Haynes 282 to achieve 100,000+ hours of life. Figure 11 shows the predicted stress distribution with exaggerated deformation and shows how the welds were placed away from the highest stress areas, especially near the struts near the inlet and exit plenum. Forgings of INCO 625 GR1 were procured for the main barrel, inlet plenum ring, and exit plenum ring. These forgings were sent to a machine shop for rough machining. The plenum rings were machined to a final shape, and the main barrel was rough cut and had the integral flow path struts machined.

After rough machining was complete, both plenum rings were welded onto the main casing along with the nozzles with full penetration welds. As with many of the other piping connections in the facility, Grayloc™ type nozzles were designed and procured due to their high temperature capability and compact size. After the completion of welding, heat treatment is performed to convert the material to grade 2. This process eliminated the weld heat-affected zone and resulted in a material better suited for temperatures above 550°C. Once welding and heat treatment were complete, the casing could be final machined. This final machining would finish off the surfaces rough cut during the initial machining and also account for any distorted areas from the welding and heat treatment processes. Once delivered, the case underwent a dual-pressure hydro test, starting with the inlet plenum, which was hydro tested in accordance with ASME. Due to the

unique geometry of the welds, 100% Radiographic Testing (RT) inspection was not possible, so a combination of RT, fracture mechanics, and hydro testing was used to qualify the casing as described in Klaerner, et al., 2023.

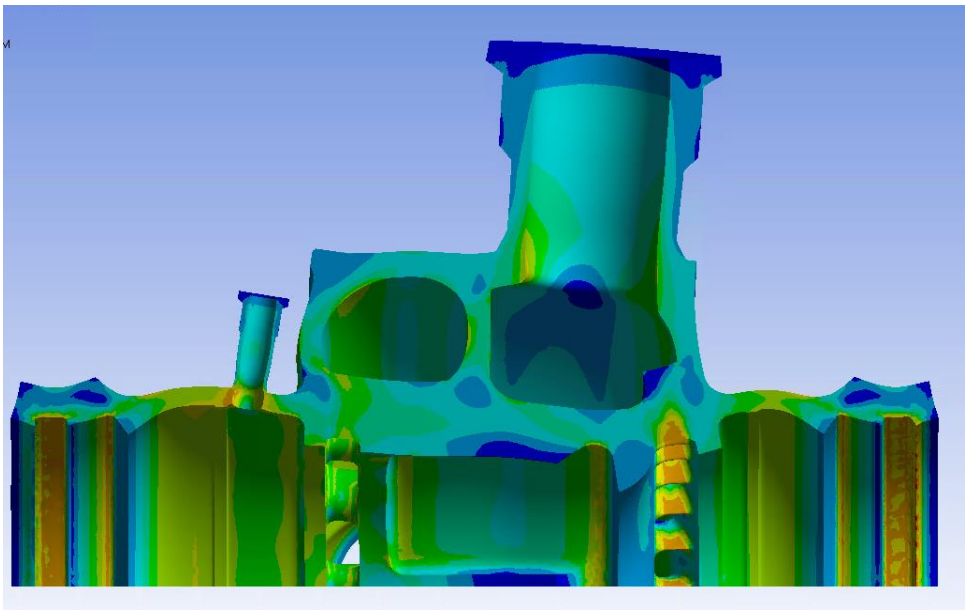

Figure 11 - Exaggerated Deformation of the Turbine and Resultant Von-Misses Stress Profile During Operating Condition

ROTOR AND STATOR MANUFACTURING

Due to the high-power density of SCO2 turbines and the relatively long flexible rotors, a monolithic design with integral shafts, blades, and shrouds was required. A Nimonic 105 rotor forging was procured, and rough turning of the shaft was performed. The airfoil shapes were cut using a 5-axis electrode discharge machining (EDM), since conventional 5-axis milling was not possible due to the close proximity of the three stages, as shown in Figure 12. A different shop was used for rotor final machining, grinding, balance, and spline addition on the shaft ends. In order to prove out the machining ability of the unique shaft splines, the splines were first cut on a sample piece of INCO 718, which resembled the machining characteristics of the Nimonic 105 but was readily available with a much shorter lead time, as shown in Figure 13. The procured couplings were test-fitted onto the spline test piece prior to giving permission for the spines to be cut on the main rotor.

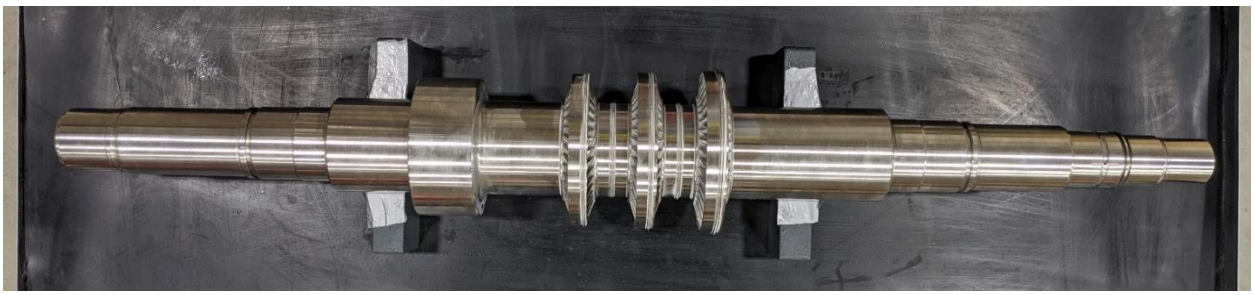

Figure 12 - Turbine rotor following rough machining and EDM

Figure 13 - Close up of EDM Turbine Blades along with Spline Test Piece

Similar to the rotor, 5-axis EDM was used to manufacture the turbine stators, followed by splitting into two halves and finishing machining (Figure 14Figure 15). A high-temperature abradable coating was applied to the stators to mate with the turbine shroud labyrinth seals to minimize internal leakage.

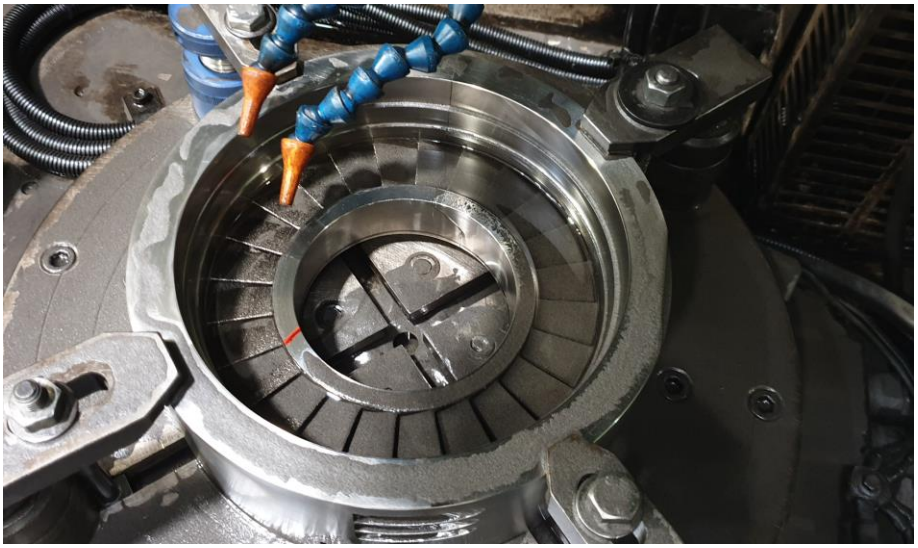

Figure 14 - Turbine Stators Being Manufactured

Figure 15 - Fully Machined Turbine Stators

TURBINE ASSEMBLY

Turbine was assembled upon receiving all the completed parts from the machine shops and following quality assurance (QA) checks. The assembly of the turbine was done on site at the STEP Facility by a team of SwRI engineers and technicians. The below sequence of illustrations in Figure 16 shows how the turbine is assembled in a vertical orientation and flipped 180 degrees to complete the assembly. Figure 17Figure 19 shows the installation of the rotor and stator assembly, the installation of the drive-end dry gas seal, and the fixture for flipping the case to assemble. The turbine was assembled while recording critical clearances and stack-ups. The turbine rotor stages are positioned correctly using adjustable shim packs as well as adjusting the thrust bearing axial end-play. Figure 20 shows the fully assembled STEP turbine next to the Sunshot turbine.

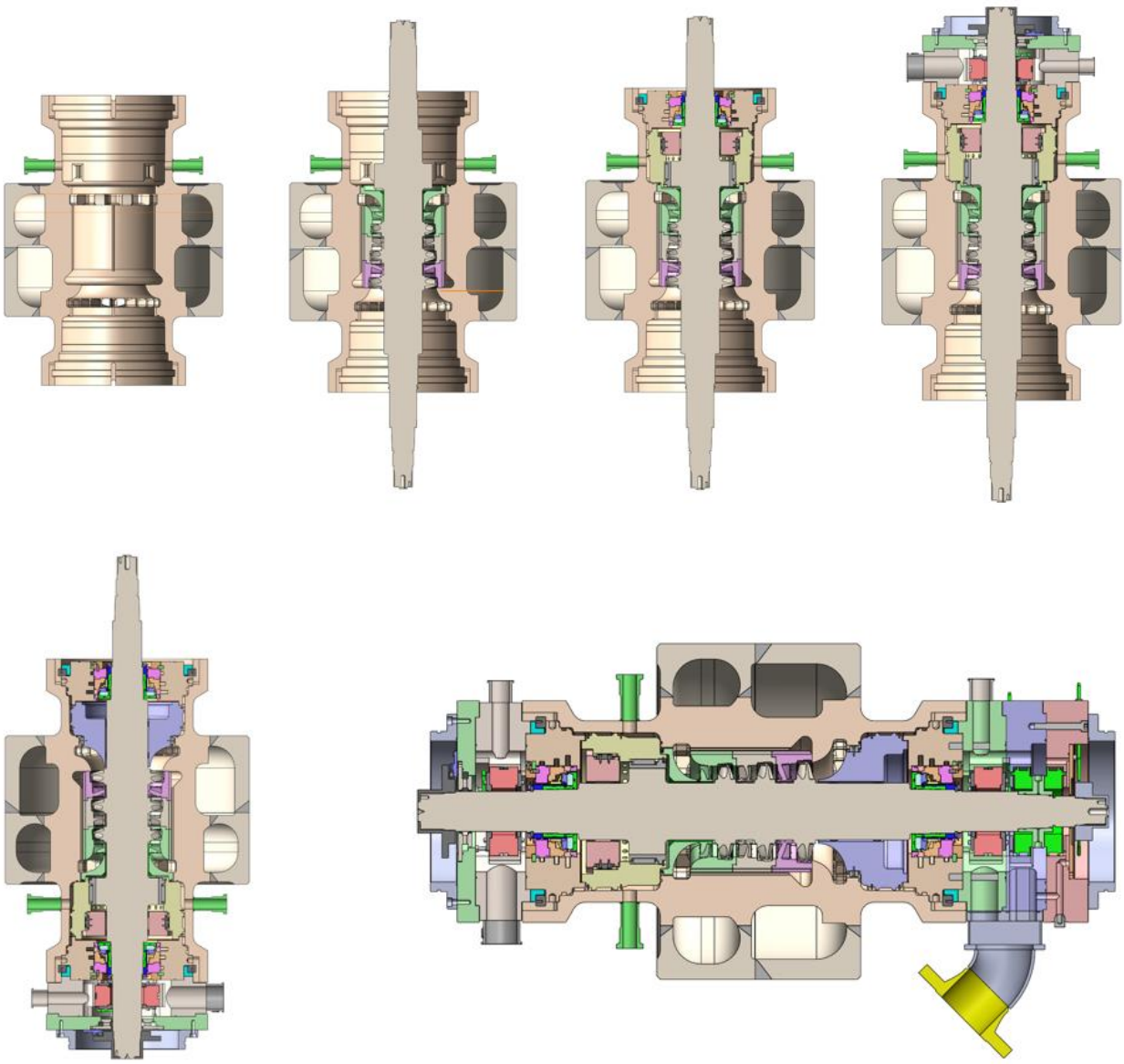

Figure 16 - Illustration of Turbine Assembly Steps

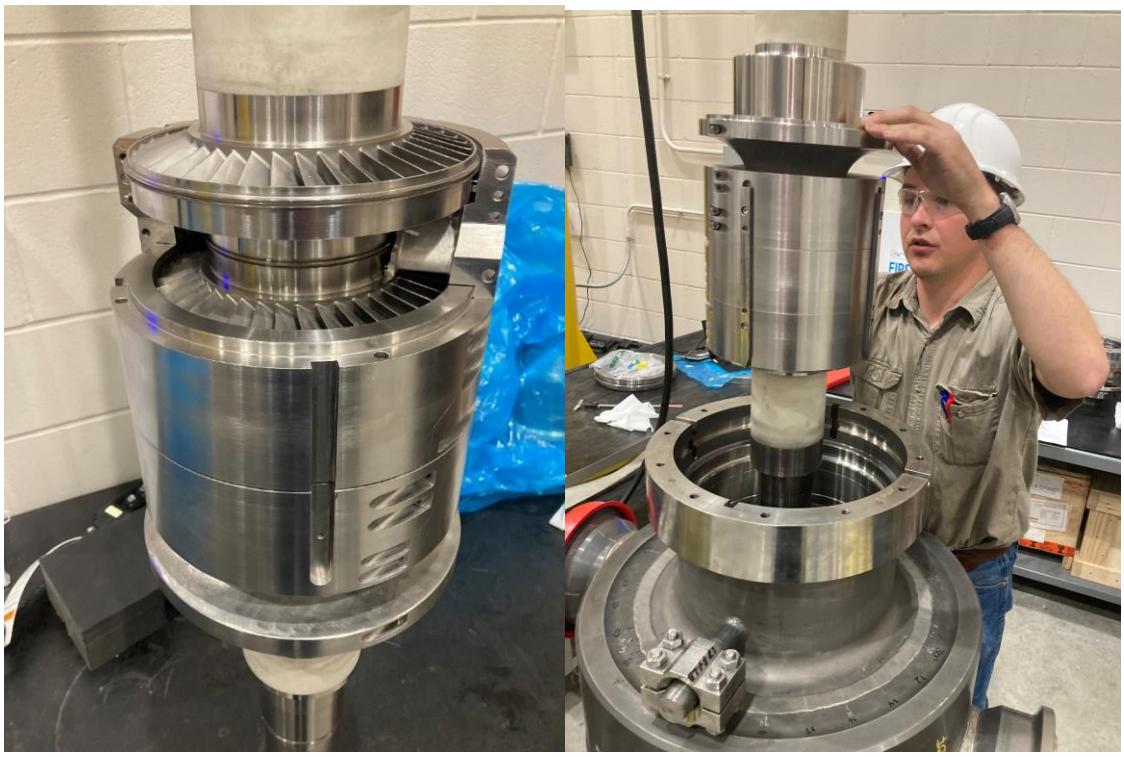

Figure 17 - Installation of Rotor/Stator Assembly into the Case

Figure 18 - Installation of Dry Gas Seal

Figure 19 - Fixture to Flip the Case

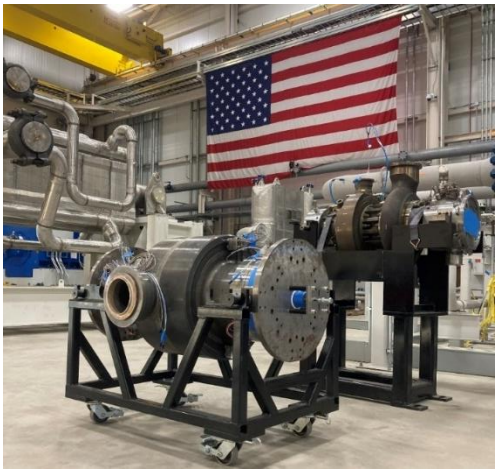

Figure 20 – Fully Assembled STEP Turbine (left) next to the Sunshot Turbine (right)

Figure 21 shows the turbine skid installed on the sub-sole plates with the generator set in place. Due to delivery delays, a rough alignment was performed between the turbine and the generator since the gearbox input and output shafts are along the same centerline. This approach permitted piping to the turbine to commence. Figure 22 shows the generator being set in place, and Figure 23 shows the high-speed coupling installed after final alignment. Cold alignment figures were calculated to account for the thermal growth of the gearbox casing. All of the machinery and instrumentation were fully wired to junction boxes and ultimately to the control panel and data acquisition systems. The fully assembled turbine skid is shown in Figure 24, representing mechanical completion.

Figure 21 - Turbine Skid with Generator Installation

Figure 22 - Gearbox Installation on Turbine Skid

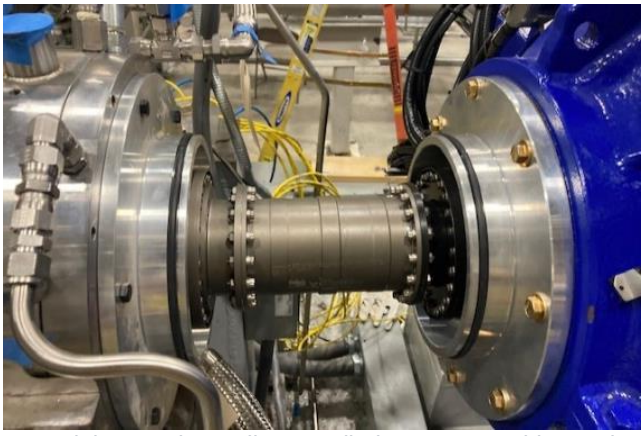

Figure 23 - High-Speed Coupling Installed Between Turbine and Gearbox

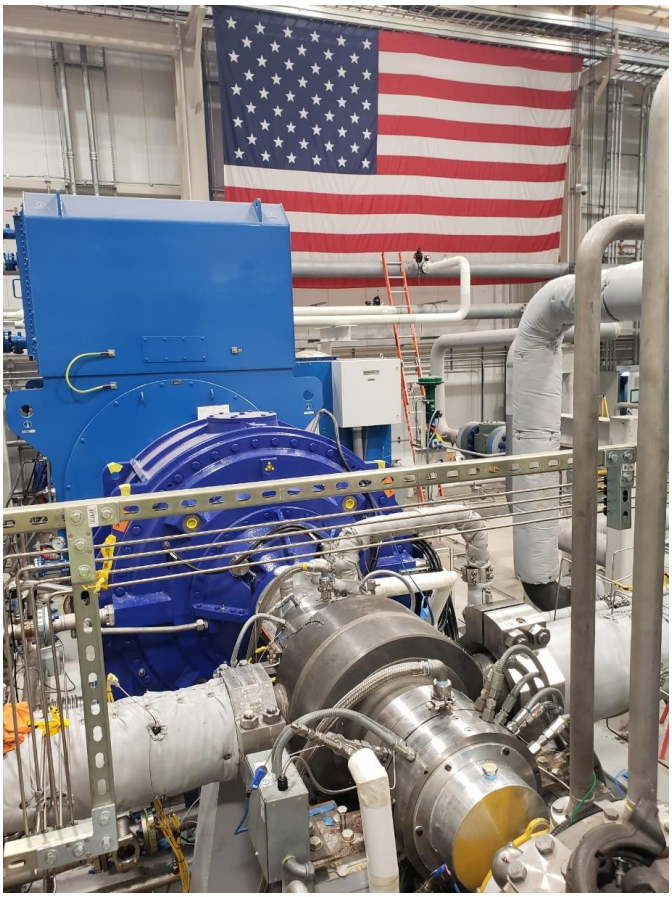

Figure 24- Fully Assembled STEP Turbine Package

MODAL TESTING

A modal test was performed on the turbine to measure the actual casing modes with all pipe connections in place. Table 1 summarizes the predicted casing modes using FEA, the rotordynamics rigid body casing model, and measured values. There are slight differences in the modeling and test assumptions. The FEA model was run without the rotor or internal stators and includes only the inlet spool pipe. The rotordynamics model has a coupled rotor and stator model, but assumes the rotor is supported on a fluid film (spinning). The modal testing was done with the inlet and exit piping connected to the casing with the rotor and other internals of the fully assembled turbine. While the rotor rests on the bearings, there is no oil film since it is not rotating but it should be representative since the squeeze film dampers control the bearing stiffness. Nonetheless, there is reasonable agreement between the two models previously shown and the measurement. Figure 25Figure 26 shows the horizontal and vertical bearing transfer functions, respectively. The results show that the modes are away from the turbine operating speed of 26,650 rpm (444 Hz) and the low-speed train (30 Hz).

Table 1 – Summary of Predicted and Measured Turbine Casing Modes

Mode Axis	Mode Type	FEA Predicted Mode Frequency (Hz)	Rotordynamics Model with Casing	*Measured Frequency (Hz)*
Horizontal	Bounce	43	127	*85*
	Conical	149		*128*
	2nd Con.		209	*216*
	Bending	615		*378*
Vertical	Bounce	102	127	*85*
	Conical	155		*129*
	2nd Con.		209	*198*
	Bending	564		*505*
Axial	Rocking	68		*85*
	Conical	157		

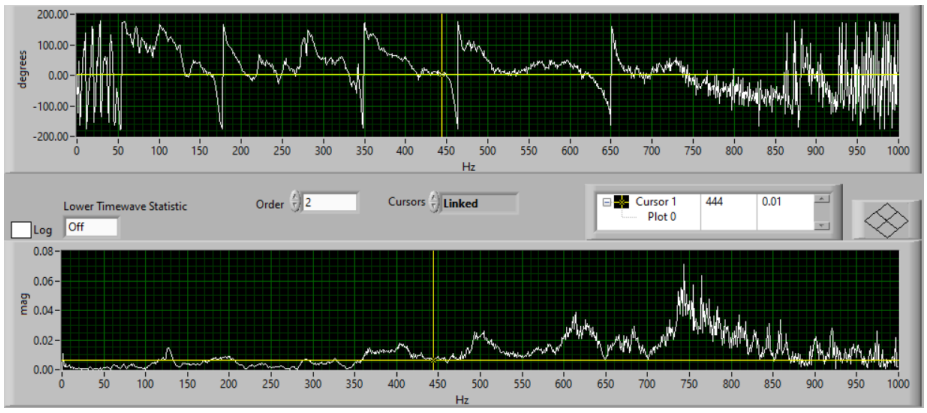

Figure 25 - Modal Test, Horizontal, DE Bearing Housing

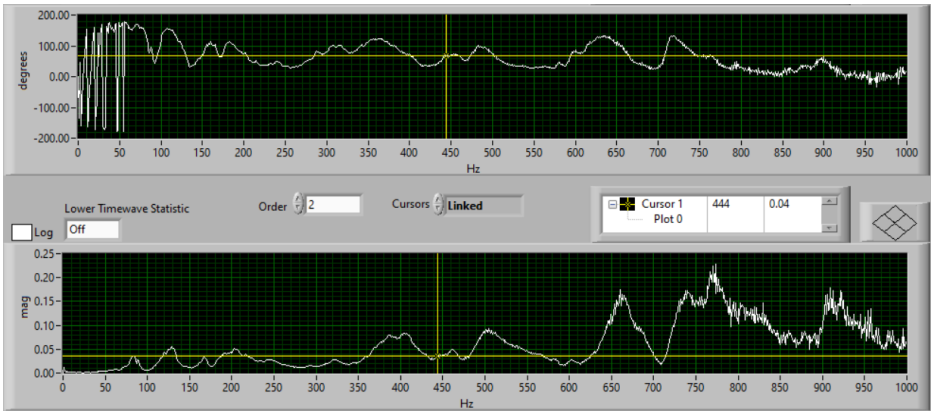

Figure 26 - Modal Test, Vertical, DE Bearing Housing

OIL SYSTEM COMMISSIONING

The turbine skid lube oil piping was designed in accordance with API 614 for supply and drain piping. The supply pipes were sized such that the flow velocities did not exceed 10 ft/s. From the supply header located on the side of the skid, the supply lines run to the bypass compressor, turbine inlet, turbine outlet, gearbox, and generator (2 connections).

Similarly, the turbine skid oil drain was sized such that the flow velocities did not exceed 0.5 ft/s. Additionally, each line was routed to slope down by 0.5 in/ft to avoid any low points anywhere in the drain piping and sized such that the oil flow in the pipe was only half-full. Sight glasses were included on each individual drain line to ensure flow during operation. Figure 27 shows the design of the lube oil piping.

Once the supply and drain piping was installed, jumpers with screens were installed between the supply and drain for each piece of equipment to bypass in accordance with API 686 guidelines. Flushing continued until screens were clean and oil samples met ISO 4406 for particle counts. The oil pipe was then connected, and oil was introduced to the equipment. Figure 28 highlights the jumpers installed.

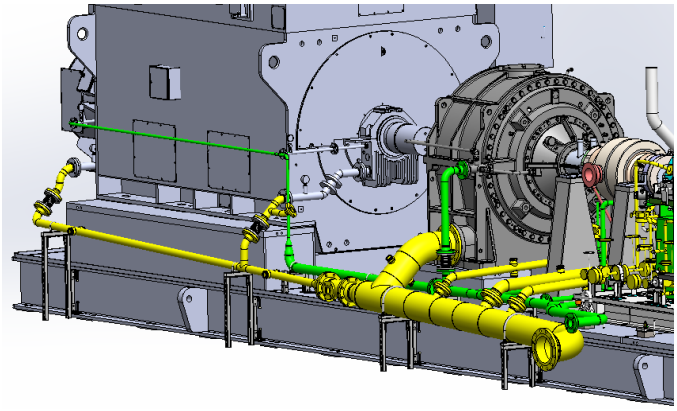

Figure 27 . Turbine Lube Oil Piping. Green Piping Indicates Supply Piping; Yellow Piping Indicates Drains.

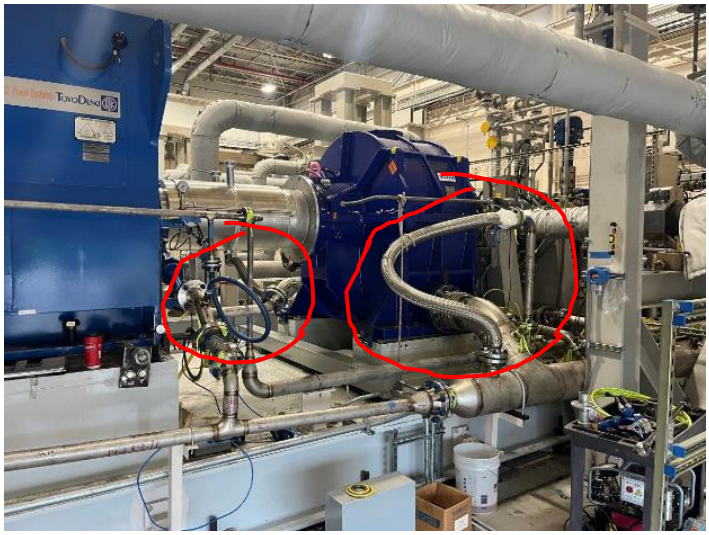

Figure 28 - Lube Oil Flushing with Jumpers Circled

SUMMARY

The STEP turbine was successfully assembled with no rework of its subcomponents, installed on the turbine skid, rough aligned, piped, final aligned, wired, and pressure checked. The ancillary systems, including the lubrication skid and dry gas seal panel, have been flushed, pressure checked, and commissioned. Instrumentation has been calibrated, including an end-to-end check of the data acquisition and control systems. The system is nearing the milestone of initial spin, which will require seal break-in, trim balancing (if required), and verification of all mechanical and vibration parameters.

The turbine design incorporated lessons learned from the Sunshot program with these enhancements: single-piece turbine case (eliminate hot casing joints and bolts), heads that use polymer seals and shear rings at the cool end of casing for better sealing, improved thermal management design to reduce shock cooling after hot shutdown, and reduced stage count from 4 to 3 with a slightly larger shaft diameter. Many features are identical to the Sunshot design, including the radial and thrust bearings, dry gas seals, balance piston seal type, and abradable labyrinths. The axial turbine design is scalable to 100+ MW. The industrial style bearings employed in STEP permit scaling to much larger values (450+MW possible). Scaling the dry gas seals to utility scale is needed and underway by other researchers. The high-power density is challenging to design a coupling that can accommodate the torque while maintaining a light weight for rotordynamics. Future publications will provide final commissioning and performance test results.

REFERENCES

American Society of Mechanical Engineers, Boiler and Pressure Vessel Code, Section VIII, Division 2, 2019.

API, 2014, Axial and Centrifugal Compressors and Expander-Compressors for Petroleum, Chemical and Gas Industry Services, API Standard 617, Eighth Edition, American Petroleum Institute, Washington, D.C.

Cich, S., Moore, J., Mortzheim, J., Singh, R., 2018, “Aeromechanical Design of a 10 MWe SCO2 Turbine,” The 7th International Supercritical CO2 Power Cycles Symposium, March 30 – April 2, 2018, San Antonio, Texas

Ertas, B., Delgado, A., and Moore, J., 2018, “Dynamic Characterization of an Integral Squeeze Film Bearing Support Damper for a Supercritical CO2 Expander,” Journal of Engineering for Gas Turbines and Power.

Klaerner, J., Moore, J., Robinson, K., Wade, J., McClung, A., 2023, “Manufacturing and Hydro Testing of a 10 MWe SCO2 Axial Turbine, Proceedings of ASME Turbo Expo 2023, Turbomachinery Technical Conference and Exposition, GT2023-103135, June 26-30, 2023, Boston, Massachusetts

Marion, J., Macadam, S., McClung, A., Mortzheim, J., “The STEP 10 MWe sCO2 Pilot Demonstration Status Update”, GT2022-83588, Proceedings of ASME Turbo Expo 2022 Turbomachinery Technical Conference and Exposition, June 13-17, 2022, Rotterdam, The Netherlands

McClung, A., Smith, N., Allison, T., and Tom, B., 2018, “Practical Considerations for the Conceptual Design of an sCO2 Cycle,” 6th International Supercritical CO2 Power Cycles Symposium, Pittsburgh, Pennsylvania, United States.

Moore, J.J., Evans, N., Brun, K., Kalra, C., 2015, “Development of 1 MWe Supercritical CO2 Test Loop,” Proceedings of the ASME Turbo Expo, Paper #GT2015-43771, June 15-19, 2015, Montreal, Quebec, Canada.

Moore, J.J., Cich, S., Day-Towler, M., Hofer, D., Mortzheim, J., 2018, “Testing of a 10 MWe Supercritical CO2 Turbine,” Proceedings of 47th Turbomachinery Symposium, Houston, TX, September 2018.

Moore, J.J., Cich, S., Day-Towler, M., Mortzheim, J., 2020, “Development and Testing of a 10 MWe Supercritical CO2 Turbine in a 1 MWe Flow Loop,” GT2020-13894, Proceedings of the ASME 2020 Turbo Expo Turbomachinery Technical Conference & Exposition, Virtual, June 22-26, 2020.

ACKNOWLDEGEMENTS

The authors would like to acknowledge and thank the hard work of the team members of GTI, SwRI, GE and Joint Industry Program members, and gratefully acknowledge the U.S. Department of Energy, Office of Fossil Energy and the National Energy Technology Laboratory, under Award Number DE-FE0028979. Special thanks to Mr. Chris Kulhanek of Southwest Research Institute for his support on the rotordynamics analysis.

DISCLAIMER